Summary

The results presented indicated that DMA is not complexed in the basic melt but forms an $AlCl_3$ adduct in the acidic melt. The formation of protonated DMA takes place in both basic and acidic melts; the reaction of DMA with proton in the basic melt appears quantitative, while in the acidic melt, where a DMA-$AlCl_3$ adduct is formed, an equilibrium between the protonated species and $AlCl_3$ adduct exists. Both electrochemistry and NMR support these observations.

Acknowledgment. This work was supported by the Air Force Office of Scientific Research. We would also like to acknowledge helpful discussions with Prof. C. D. Ritchie.

Electrochemistry at the Air/Water Interface. Lateral Diffusion of an Octadecylferrocene Amphiphile in Langmuir Monolayers

Deborah H. Charych, Ehud M. Landau, and Marcin Majda*

Contribution from the Department of Chemistry, University of California, Berkeley, Berkeley, California 94720. *Received October 10, 1990*

Abstract: A new electrochemical method is described to investigate the dynamics of lateral diffusion processes in Langmuir monolayers at the air/water interface. The key element of this technique is a gold microband electrode, which can be positioned in the plane of the water surface and which functions as a 1D electrode in contact with a 2D collection of electroactive, water insoluble molecules. Investigations of *N*-octadecylferrocenecarboxamide ($C_{18}Fc$) monolayers and mixed monolayers of $C_{18}Fc$ and octadecanol on 0.05 M $HClO_4$ at 28 °C showed that they remain fluid without undergoing any phase transitions, in a surface concentration range of 3.3×10^{-10} to 7×10^{-11} mol/cm^2. Lateral diffusion of $C_{18}Fc$ can be modeled as a 2D fluid of hard disks with the cross sectional area equal to the projected area of the ferrocene head group. The diffusion coefficient increases linearly with the average free area per molecule on the water surface.

Introduction

This report is concerned with the dynamics of molecular diffusion in 2D systems of Langmuir monolayers at the air/water interface. Our experimental approach is based on electrochemical techniques and relies on a purposefully designed microelectrode, which is positioned in the plane of the air/water interface and which acts as a 1D electrode in this 2D electrochemical experiment. The measurements reported below contribute to the understanding of lateral transport processes and fluidity of biological membranes.[1] In addition, our electrochemical method is capable of providing insight into the kinetics of lateral electron hopping in monolayer assemblies at the air/water interface.

Electrochemical methods are very well suited for the investigation of the dynamics of transport processes, since Faradaic current, even at modest overpotentials, is directly proportional to the arrival rate of the electrochemically active molecules at the electrode surface.[2] We have recently shown the application of electrochemical methods in studies of the lateral diffusion of amphiphiles in organized bilayers produced by self-assembly techniques at Al_2O_3 or glass surfaces.[3,4] The key element in those studies was the development of experimental techniques that allow one to position a working electrode perpendicular to a bilayer assembly. Under such conditions, current can be interpreted in terms of the dynamics of the lateral processes in the bilayer. In this report, we use a similar electrochemical approach to investigate lateral diffusion of a water insoluble *N*-octadecylferrocenecarboxamide ($C_{18}Fc$) at the air/water interface under controlled surface pressure conditions. As in the previous cases, the particular design of a microelectrode that can be positioned at the air/water interface to be perpendicular to the $C_{18}Fc$ monolayer is the key feature of the experiment.

The perpendicular orientation of the microelectrode to the air/water interface is accomplished by creating a sharp gradient of wettability along a single line on a gold surface. The key elements of the microelectrode design and its positioning at the air/water interface are shown in Figure 1. The microelectrodes are fabricated by vapor deposition of narrow strips of gold onto glass slides (see Experimental Section). Subsequently, all gold and glass surfaces were rendered hydrophobic by self-assembly of a long hydrocarbon chain monolayer. Prior to an electrochemical experiment, a gold-coated substrate is fractured in half, along a line perpendicular to the gold strip. This produces two microband electrodes with freshly exposed microbands of gold at the edge of each half of the glass slide. One microband electrode is then positioned at the air/water interface with the freshly created edge now in contact with water as shown in Figure 1. The high gradient of wettability between the clean, hydrophilic gold of the microband and the monolayer-coated, hydrophobic gold surface defines, along a single line, the coexistence front of three phases. It is this line that plays a role of a 1D electrode addressing a monolayer at the air/water interface. The reduction of dimensionality in this 2D electrochemical experiment does not affect the shape of the current voltage curves, as we demonstrate below.

Electrochemical methods have been used previously in the investigations of monolayers at the air/water interface.[5] However, the method described here is unique in that it directly probes the dynamics of the *lateral* diffusion processes in monolayers at the water surface. To this extent, our method parallels fluorescence microphotolysis (fluorescence recovery after photobleaching), which has been used extensively in the investigations of lateral

(1) Cadenhead, D. A. In *Structure and Properties of Cell Membranes*; Benga, G., Ed.; CRC Press: Boca Raton, FL, 1985; Vol. 3, p 21.
(2) Bard, A. J.; Faulkner, L. R. *Electrochemical Methods. Fundamentals and Applications*; Wiley: New York, 1980; Chapter 1.
(3) (a) Miller, C. J.; Widrig, C. A.; Charych, D. H.; Majda, M. *J. Phys. Chem.* **1988**, *92*, 1928. (b) Goss, C. A.; Miller, C. J.; Majda, M. *J. Phys. Chem.* **1988**, *92*, 1937. (c) Miller, C. J.; Majda, M. *Anal. Chem.* **1988**, *60*, 1168. (d) Bourdillon, C.; Majda, M. *J. Am. Chem. Soc.* **1990**, *112*, 1795.
(4) Goss, C. A.; Majda, M. *J. Electroanal. Chem.* **1991**, *300*, 377.
(5) (a) Fujihira, M.; Araki, T. *Chem. Lett.* **1986**, 921. (b) Zhang, X.; Bard, A. J. *J. Am. Chem. Soc.* **1989**, *111*, 8098.

0002-7863/91/1513-3340$02.50/0

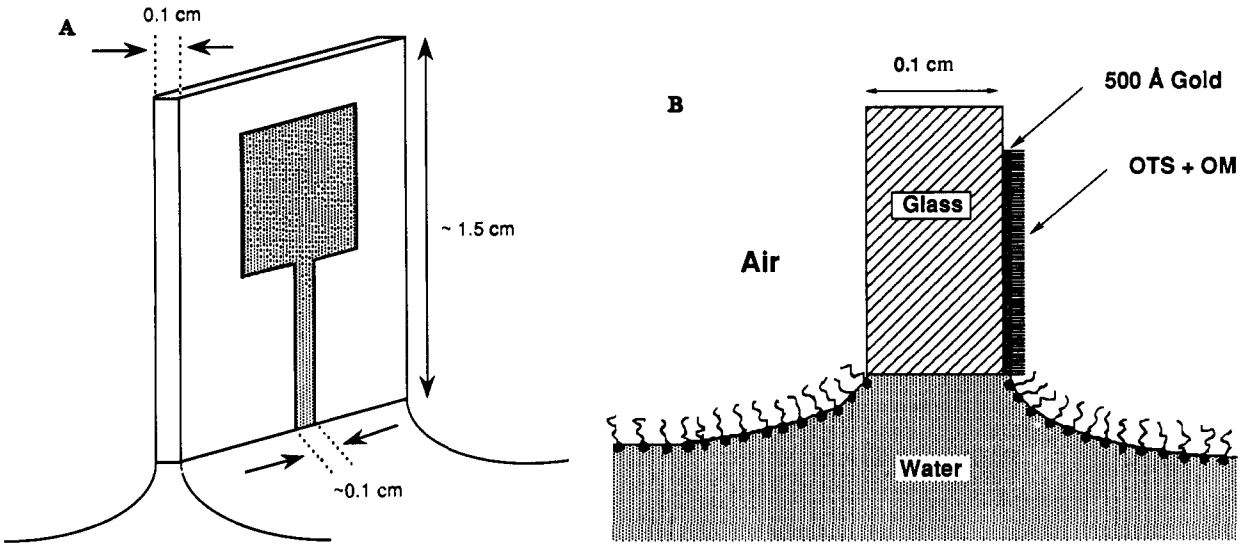

Figure 1. Microband electrode and its positioning at the air/water interface. (A) A glass slide with the vapor-deposited gold film (marked by the shaded area) is held above the water surface. Water forms a positive meniscus by wetting the bottom edge of the glass slide. The electrical contact (not shown) is formed in the upper section of the gold pattern. The 1D electrode is the 0.1-cm-long line in the plane of the water surface, defined by the difference in wettability of the clean gold edge and of the OM-coated gold surface above the water, as shown in part B. (B) A schematic (out of scale) cross-sectional side-view of the microband electrode at the air/water interface. The bottom edge of the glass slide (including the gold film) in contact with water was created by breaking in half a gold-coated glass slide, which initially carried a twin-pair electrode pattern (see Experimental Section). All gold and glass surfaces of the glass slide shown in part A are nonwettable, since they are coated by a self-assembled monolayer of octadecanethiol and octadecyltrichlorosilane. For simplicity, the OTS + OM monolayer is shown on the gold surface only. The amphiphilic molecules on the water surface represent $C_{18}Fc$.

diffusion of phospholipids and proteins in bilayer membranes and their model systems.[6] Preliminary results of our electrochemical method have been published previously.[7]

In this report, we examine the dependence of the $C_{18}Fc$ lateral diffusion coefficient at the air/water interface on its surface concentration. In the region of surface concentrations from ca. 7×10^{-11} to 3.3×10^{-10} mol/cm^2 (the concentration of fully packed $C_{18}Fc$ monolayer is 3.6×10^{-10} mol/cm^2), the $C_{18}Fc$ diffusion coefficient is directly proportional to the void area in the surface monolayer. This is in agreement with the Cohen–Turnbull model of diffusion in hard-sphere fluids.[8] The diffusion coefficient decreases from ca. 5×10^{-6} to 2×10^{-7} cm^2/s as the void area varies from 200 to 4 Å^2/molecule (the projected area of $C_{18}Fc$ is 46 Å^2/molecule). The measurements were done at 28 °C, where the $C_{18}Fc$ monolayer does not exhibit any phase transitions within the range of concentrations just mentioned.

Experimental Section

Materials. *N*-octadecylferrocenecarboxamide ($C_{18}Fc$) was synthesized by reacting octadecylamine with ferrocenecarboxylic acid chloride. Ferrocenecarboxylic acid (4 g, 17.4 mmol) was dissolved in warm (50 °C) PCl_3 and stirred overnight. The excess PCl_3 was removed by rotary evaporation under reduced pressure. The acid chloride was purified twice by dissolving it in approximately 30–40 mL of boiling petroleum ether, filtering out any precipitate, and recovering the compound from the filtrate by rotary evaporation at a reduced pressure. The acid chloride was then dissolved in ca. 100 mL of dry THF in a single-neck, round-bottom flask and combined with a 2-fold excess of octadecylamine dissolved in dry THF. When these two clear solutions were mixed, some octadecylammonium chloride precipitated immediately. The solution was stirred for 1 h at room temperature, the yellow-white precipitate filtered, and the crude light yellow product recovered after rotary evaporation. The product was then purified by flash chromatography (silica gel, 230–400 mesh, 60 Å; eluted with 9:1 $CHCl_3/CH_3OH$). The purity of $C_{18}Fc$ was determined by TLC (UV, I_2, and ninhydrin tests), NMR, and elemental analysis: ^{1}H NMR (250 MHz, $CDCl_3$) δ 0.88 (t, 3 H, CH_3), 1.30 (s, 32 H, CH_2), 3.35 (q, 2 H, CH_2CH_2NH), 4.20 (s, 5 H, Cp), 4.30 (m, 2 H, Cp), 5.65 (t, 1 H, CH_2NH). Anal. Calcd: C, 72.3; H, 9.8; N, 2.9. Found: C, 72.4; H, 9.9; N, 2.9.

House-distilled H_2O was passed through a four-cartridge Barnstead Nanopure II purification train consisting of Macropure pretreatment, Organics Free for removing trace organics, two ion exchangers, and a 0.2 μM hollow-fiber final filter for removing particles. Its resistivity was 18.3 MΩ cm. Octadecyltrichlorosilane (OTS) and (3-mercaptopropyl)trimethoxysilane were from Petrarch Systems Inc. OTS was vacuum-distilled into sealed glass ampules, which were opened as needed immediately prior to the individual experiments. Octadecanol (Aldrich, 99%) and octadecanethiol (OM) (Aldrich, 98%) were recrystallized from 95% ethanol. Reagent-grade 70% $HClO_4$ (Aldrich), chloroform (Fisher, ACS certified spectranalyzed), methanol (Fisher, spectroscopic grade), lead nitrate (Mallinckrodt), and all the other reagents were used as received.

Monolayer Techniques. The experiments at the air/water interface were carried out in a standard Langmuir trough (45 × 15 cm, KSV Model 2200) equipped with a surface pressure microbalance with the Wilhelmy plate technique. The instrument was controlled by a PC AT clone computer and KSV Dynamic Film Control System Software Version 2.0. In order to isolate the instrument from the dust in the laboratory air, the Langmuir trough and all the accessories except the external electronic and computer control units were completely enclosed in a Plexiglass box equipped with the hand-entry iris ports. Electrical cables, electrode leads, and plastic tubings for aspiration and thermostating were brought into the box via nylon or brass Swagelok fittings. The box was continuously purged with filtered (0.01 μm Matheson membrane gas filter) nitrogen to maintain purity of atmosphere and to lower relative humidity below ca. 75%. We consistently found that the electrochemical experiments at the air/water interface became irreproducible when gas in the Plexiglass box that houses the Langmuir trough was saturated with water. (Occasionally, clean air or Ar was used instead of N_2, with no effect on the experimental results.) Periodically, the box was thoroughly vacuum-cleaned and scrubbed with 2-propanol. Hands entering the iris ports were covered with OAK Technical long-length powder-free vinyl gloves used in Class 100 clean rooms. We want to stress that all these precautions to isolate the instrument from the environmental sources of contamination were necessary to achieve reproducible working conditions where a Langmuir monolayer could be examined for a substantial length of time (ca. 1 h) without showing deterioration in the electrochemical measurements.

The Langmuir trough was periodically cleaned with fresh chromic acid solution followed by repeated rinsing with pure water and then it was soaked in HPLC-grade chloroform, wiped with Techni-Cloth texwipes (Class 100 clean room grade), and soaked again in spectroscopic-grade

(6) (a) Peters, R. *Cell Biol. Int. Rep.* **1981**, *5*, 733. (b) Edidin, M. In *Membrane Structure*; Finean, J. B., Michell, R. H., Eds.: Elsevier: New York, 1981; Chapter 2, p 37. (c) Vaz, W.; Derko, Z. I.; Jacobson, K. A. *Cell Surf. Rev.* **1982**, *8*, 83. (d) Wade, C. G. In *Structure and Properties of Cell Membranes*; Benga, G., Ed.; CRC Press: 1985; Vol. 1, p 51.

(7) Widrig, C. A.; Miller, C. J.; Majda, M. *J. Am. Chem. Soc.* **1988**, *110*, 2009.

(8) (a) Cohen, M. H.; Turnbull, D. *J. Chem. Phys.* **1959**, *31*, 1164. (b) Turnbull, D.; Cohen, M. H. *J. Chem. Phys.* **1970**, *52*, 3038.

methanol and finally in pure water. A platinum Wilhelmy plate used in the surface pressure measurements was cleaned after each experiment in fresh, hot chromic acid solution and rinsed thoroughly with pure water. Identical surface pressure results were also obtained when acid-washed filter paper was used as the Wilhelmy plate.

The monolayer spreading solutions (ca. 2 μmol/mL) were prepared fresh daily by weighing and dissolving an appropriate amount of a surfactant in chloroform. Purity of the chloroform was checked by spreading 100–200-μL aliquots on the clean surface, sweeping the barrier, and measuring the surface pressure. Pure solvents gave no detectable rise in the surface pressure. To spread a surface monolayer of a surfactant, a 20–40-μL aliquot of a spreading solution was delivered in different locations to the subphase surface with a Hamilton gas-tight microliter syringe. The initial trough area was typically 500 cm^2. The surface films were compressed at a rate of 10 ($Å^2$/molecule)/min. Increasing or decreasing the compression rate by a factor of 2 had no effect on the surface pressure isotherms. After each experiment, the surface monolayer was aspirated following its compression to a small area. The expansion, compression, and aspiration cycle was repeated two more times, and then the cleanliness of the subphase surface was checked, as described above, before the next Langmuir monolayer could be spread.

Fabrication of the Microband Electrodes. The electrodes were produced by gold vacuum deposition on standard 3 × 1 in. glass microscope slides. In order to achieve the desired background characteristics of the microband electrodes, the usual 50–70-Å chromium underlayer was replaced by a surface film of (3-mercaptopropyl)trimethoxysilane, as described elsewhere,[9] as a means of improving gold adhesion to the glass surface. Metal masks were used to define the electrode pattern. This consists of two rectangular contact pads of ca. 0.5 cm^2 in an area linked by a ca. 0.1-cm-wide and 1.5-cm-long strip. This defined a twin pair of electrodes, which ultimately were obtained by fracturing the gold-coated glass substrate along a line perpendicular to the gold strip approximately halfway between the contact pads. Typically, about 500–800-Å gold (99.999% Lawrence Berkeley Laboratory) films were deposited (measured with a quartz crystal thickness monitor by Kronos Inc.) in a Veeco Model 7700 bell jar operating at 2 × 10^{-7} Torr of base pressure. Adhesion of the gold to the glass surface, which is a prerequisite for well-functioning microband electrodes, was considered acceptable if a piece of adhesive tape (Scotch, Magic Transparent), firmly placed over the Au film and the surrounding glass surface, could be removed without removing any of the evaporated gold film.[9] Electrode substrates were subsequently immersed in a solution of 40 mM octadecanethiol in toluene for 45 min to 2 h, rinsed with toluene, dried with a stream of Ar, rinsed with water, and dried again. They were then placed in a ca. 2% solution of octadecyltrichlorosilane in hexadecane for 20–30 min, rinsed with toluene, and dried. The advancing contact angles of water were typically 112–114° on the gold and 111–113° on the glass. Silver epoxy (Epo-Tek 415G) was applied to each rectangular contact pad of the twin electrode pair, and the electrodes were cured overnight at 70 °C. The 1 × 3 in. substrates were then cut into sections containing individual twin electrode pairs. Individual electrode substrates were scribed on the back with a diamond pencil and fractured just before an electrochemical experiment. After fracturing, the electrodes did not deteriorate for at least several hours when kept in the box of the Langmuir trough or in a laminar flow hood.

Electrochemical Experiments. Cyclic voltammetric and chronoamperometric experiments were done with an EG&G PAR Model 175 universal programmer and a locally constructed Model 852 bipotentiostat (R. Ensman, Indiana University). In the chronoamperometric experiments, the data were acquired by a PC AT clone computer with use of a Labmaster DMA A/D converter. Asyst software (Rochester, NY) was used for data collection and analysis.

Individual gold microband electrodes were positioned on the clean subphase surface with the aid of a motorized lifter to create a positive water meniscus at the electrode edge (see Figure 1). The reference electrode (Radiometer Model K401 SCE) and Pt counter electrode were positioned behind the barrier of the Langmuir trough (see Figure 3). After the background current was recorded, the working electrode was lifted up, the monolayer was spread as described above, and the microband electrode was carefully repositioned on the air/water interface. The same electrode could be used for a number of voltammetric and chronoamperometric experiments at various $C_{18}Fc$ surface concentrations. Experiments with a particular electrode were discontinued whenever chronoamperometric Cottrell plots became nonlinear. The electrode length was measured after each experiment with ±0.01-cm precision with use of light microscope equipped with a filar micrometer. The thickness of the gold films on glass was measured with a stylus profilometer (Alpha Step 100, Tencor, Inc.).

(9) Goss, C. A.; Charych, D. H.; Majda, M. *Anal. Chem.* **1991**, *63*, 85.

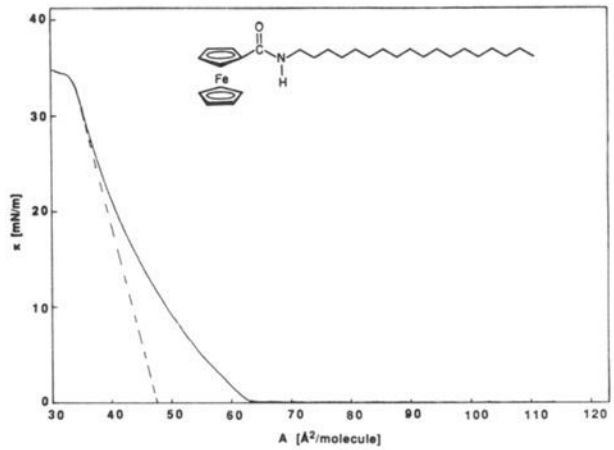

Figure 2. Structural formula and a π–A isotherm of $C_{18}Fc$ recorded on 0.05 M $HClO_4$ subphase at 28 °C. The average area per molecule obtained by extrapolation of the steepest part of the isotherm to $\pi = 0$ is 48 ± 2 $Å^2$/molecule.

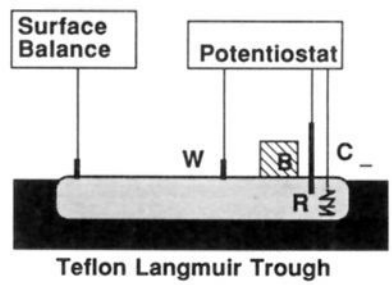

Figure 3. Schematic diagram showing the experimental setup used in the 2D electrochemical measurements: W, working microband electrode touching the water surface (see Figure 1 for more detail); B, moveable barrier of the Langmuir trough; R, reference electrode; C, counter electrode.

Results and Discussion

$C_{18}Fc$ Behavior at the Air/Water Interface. The chemical structure of $C_{18}Fc$ is shown in Figure 2 together with its surface pressure–area (π–A) diagram recorded on the 0.05 M $HClO_4$ subphase at 28 °C. The shape of the π–A isotherm shows no phase transitions in the liquid region, where measurable surface pressure can be recorded. The monolayer collapses above ca. 33 mN/m. The $C_{18}Fc$ limiting area obtained by extrapolating the steepest part of the isotherm to $\pi = 0$ is 48 ± 2 $Å^2$/molecule. This value is consistent with the cross-sectional area of the ferrocene head group of $C_{18}Fc$. The limiting area and the shape of the isotherm are independent of the perchloric acid concentration unless it is increased to ca. 1 M, when the limiting area increases to ca. 53 $Å^2$/molecule. This effect may be caused by partial protonation of the iron in ferrocene, which is known to occur in concentrated solutions of strong acids.[10] The resulting Coulombic repulsion is then responsible for the observed shift in the π–A isotherm.

Electrochemical Experiments at the Air/Water Interface. The electrochemical experiments were carried out on the Langmuir trough as shown schematically in Figure 3. The key element in the design of the microelectrode shown in Figure 1 is the creation of the sharply defined interface between wettable and nonwettable gold surfaces. This is accomplished by fracturing a glass/Au slide coated with a monolayer of octadecanethiol and octadecyltrichlorosilane molecules (see Experimental Section). When positioned at the air/water interface as shown in Figure 1, the microband electrode creates a hemicylindrical diffusion zone during reduction of electroactive species in the electrolyte. As expected,

(10) (a) Curphey, T. J.; Santer, J. O.; Rosenblum, M.; Richards, J. H. *J. Am. Chem. Soc.* **1960**, *82*, 5249. (b) Ballhausen, C. J.; Dahl, J. P. *Acta Chem. Scand.* **1961**, *15*, 1333. (c) Cerichelli, G.; Illuminati, G.; Ortaggi, G. *J. Organomet. Chem.* **1977**, *127*, 357.

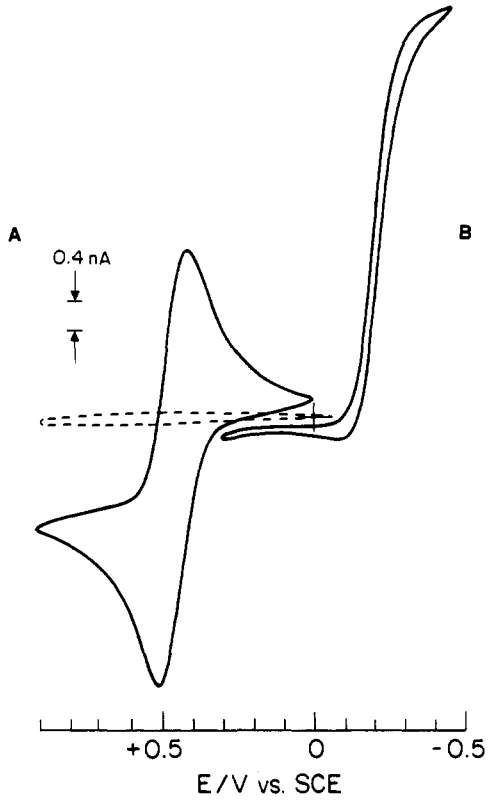

Figure 4. Cyclic voltammograms recorded at a gold microband electrode positioned at the air/water interface as shown in Figure 1. Curve A: continuous line, 1.38×10^{-10} mol/cm^2 $C_{18}Fc$ (120 Å^2/molecule) on 0.05 M $HClO_4$ subphase; dashed line, background recorded on the same electrode before $C_{18}Fc$ monolayer was spread on water surface; T = 27 °C, l = 0.158 cm, v = 200 mV/s. Curve B: clean water surface; 7×10^{-4} M $Ru(NH_3)_6^{3+}$ in 0.5 M KCl; l = 0.158 cm, w = 500 Å, v = 100 mV/s.

this generates sigmoidal-type voltammograms as shown in Figure 4 (curve B) for the reduction of $Ru(NH_3)_6^{3+}$ ions.[11] However, when the electroactive molecules such as $C_{18}Fc$ are restricted to the air/water interface, the gold microband acts as a 1D electrode lying in the plane of the air/water interface. Diffusion to this line electrode occurs, on a voltammetric time scale, according to the linear diffusion pattern in 2D. Hence, the shape of the 2D voltammograms (i.e., those addressing 2D systems of electroactive species) could be expected to be identical with those in classical voltammetric experiments. Our experiments confirm this expectation (see Figure 4, curve A). It appears that the reduction of dimensionality requires only that the product of electrode surface area and the initial concentration of the electroactive species in the voltammetric equation is replaced by the product of the electrode length (l) and the surface concentration (Γ^*). (This does not affect the unit of the product, which remains mol/cm.) Thus, one obtains[12]

$$i = nFl\Gamma^*(\pi D\sigma)^{1/2}\chi(\sigma t) \qquad (1)$$

where D is the 2D diffusion coefficient (cm^2/s), $\sigma = nFv/RT$, v is the electrode potential scan rate, and $\chi(\sigma t)$ is the usual, linear-sweep voltammetric current function.[12]

The shape of the 2D cyclic voltammetric curve in Figure 4, curve A, is indeed consistent with this model. The peak to peak separation is ca. 95 mV, suggesting the presence of uncompensated resistance and/or quasi-reversible character of the heterogeneous electron transfer. The anodic and cathodic peak currents are equal in height and both exhibit linear dependence on $v^{1/2}$ with zero intercept (r = 0.998 in the scan range of 50–1000 mV/s). This

(11) Wightman, R. M.; Wipf, D. O. In *Electroanalytical Chemistry*; Bard, A. J., Ed.; Dekker: New York, 1989; Vol. 15, p 267.
(12) Bard, A. J.; Faulkner, L. R. *Electrochemical Methods. Fundamentals and Applications*; Wiley: New York, 1980; Chapters 5–6.

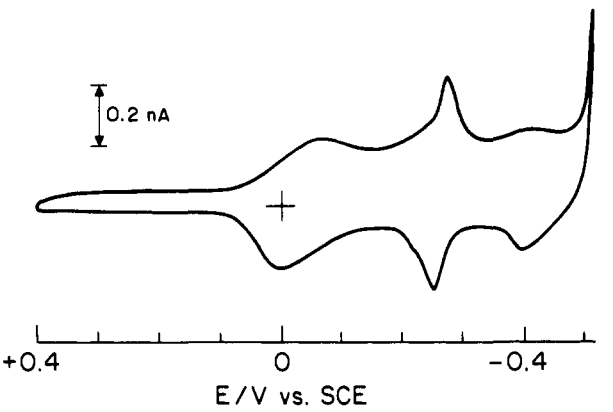

Figure 5. Cyclic voltammogram of Pb^{2+} UPD on a gold microband electrode positioned at the air/water interface as shown in Figure 1. $PbNO_3$ (1.0 mM) in 1.0 M $HClO_4$: $A = 7.35 \times 10^{-7}$ cm^2 (l = 0.147 cm, w = 500 Å); v = 100 mV/s.

confirms the purely diffusional character of these voltammograms. Since the gold microband functions as a 1D electrode in this experiment, the magnitude of the 2D voltammetric peak current is independent of the width of the microband and depends linearly on its length only. Under the conditions of Figure 4, the 2D current density was 1.96 ± 0.08 nA/cm. This represents an average of over 15 measurements carried out at different electrodes 500, 1000, and 2100 Å in width.

The values of the widths of the microband electrodes quoted above are the nominal values, obtained from measurements of the thickness of the vapor-deposited gold films by stylus profilometry. The actual surface area of gold created by fracturing a gold-coated glass slide depends on the mechanics of the breaking process and the extent of damage such a process might induce in a thin gold film near the line of fracture. In order to assess the extent of possible damage, we carried out a series of lead underpotential deposition (UPD) experiments on the freshly fabricated microband electrodes, in which the electrode was positioned as in Figure 1 at the clean surface of a 1 mM $PbNO_3$/1 M $HClO_4$ solution. A representative Pb UPD voltammogram is shown in Figure 5. Its shape is consistent with published Pb UPD results for polycrystalline gold surfaces.[13] Taking 293 μC/cm^2 as a charge of a single hexagonal close-packed layer of Pb,[14] we obtained an average value for the ratio of the UPD-determined surface area of a gold microband to its expected geometric area of 1.12 ± 0.18, based on the measurements with nine different electrodes. Thus, it appears that there is little or no damage done to the gold layer during fracturing.

To assure that no component of the 2D Faradaic current was due to the $C_{18}Fc$ absorbed or transferred to the microband electrode, the electrodes were periodically detached from the air/water interface and repositioned on the water surface behind the barrier of the Langmuir trough. The obtained background current was identical with that observed at a fresh electrode before the spreading of the monolayer (see Figure 4). However, some quantity of $C_{18}Fc$ was transferred to the microband electrode whenever the $C_{18}Fc$ monolayer was compressed above ca. 10 mN/m. This resulted in distortions of the voltammetric curves. In those cases, when the microelectrode was transferred to the clean water surface behind the barrier, $C_{18}Fc$ Faradaic current could be observed. The data presented below are, therefore, limited to surface pressures below 10 mN/m.

Lateral Diffusion of $C_{18}Fc$ at the Air/Water Interface. The diffusion coefficients of $C_{18}Fc$ at the air/water interface were obtained from a series of chronoamperometric experiments in which current is expressed by the following equation:[12]

$$i = nFl\Gamma^*D^{1/2}/(\pi t)^{1/2} \qquad (2)$$

The calculation of D values from the slope of i vs $t^{-1/2}$ plots provides

(13) Deakin, M. R.; Melroy, O. *J. Electroanal. Chem.* **1988**, *239*, 321.
(14) Schultze, J. W.; Dickertmann, D. *Surf. Sci.* **1976**, *54*, 489.

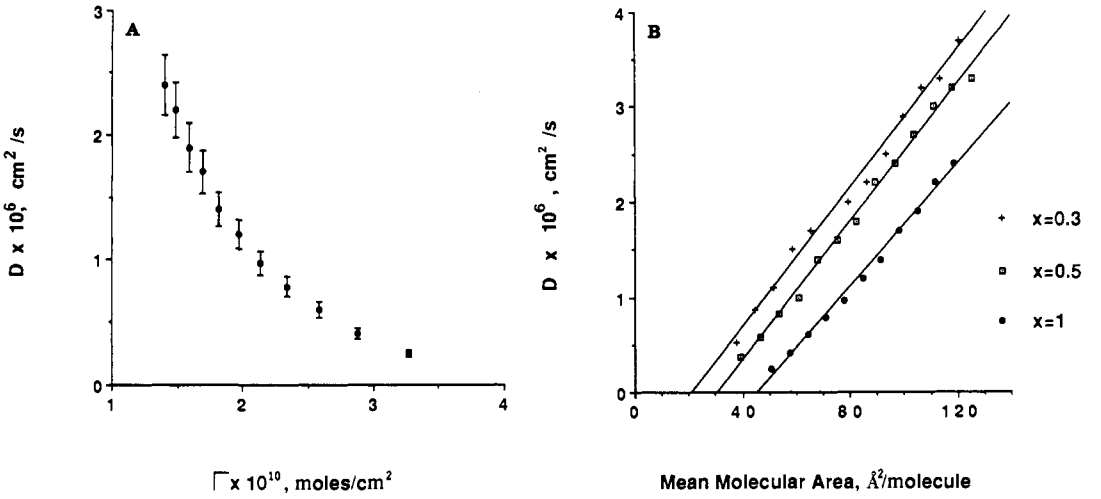

Figure 6. (A) Plot of $C_{18}Fc$ lateral diffusion coefficient at the air/water interface vs $C_{18}Fc$ surface concentration; an average error bar is ±10% of D. (B) Plots of the $C_{18}Fc$ lateral diffusion coefficients at the air/water interface vs average area per molecule. The three series of experiments correspond to pure ($C_{18}Fc$) and mixed monolayers ($C_{18}Fc$ + $C_{18}OH$) with the mole fraction of $C_{18}Fc$ noted in the figure.

an additional means of discriminating against any contributions to the Faradaic current due to material immobilized at the electrode surface. Linear i vs $t^{-1/2}$ plots were obtained in the entire time window investigated (35 ms to 5 s). The plot of D vs surface concentration of $C_{18}Fc$ at the air/water interface is shown in Figure 6A. The observed decrease in D is an expected reflection of the decreasing fuidity of the monolayer assembly. In Figure 6B, these data are replotted as D vs A, the average area per molecule. The linear extrapolation of the data to $D = 0$ gives a limiting area per molecule (A_0 = 45.8 Å^2). This value is slightly lower than that obtained from the π–A isotherm in Figure 2. The difference stems, most likely, from the fact that the $C_{18}Fc$ monolayer cannot be compressed to a fully condensed state before it collapses at ca. 30 mN/m. Also shown in Figure 6B are the results of two additional series of experiments where the $C_{18}Fc$ molecules were diluted at the air/water interface with octadecyl alcohol ($C_{18}OH$), a nonelectroactive surfactant. Diffusion of $C_{18}Fc$ still follows a linear dependence on the average area per molecule, regardless of its mole fraction ($x_{C_{18}Fc}$ of 0.5 and 0.3 were examined). Analysis of the π–A isotherms of the mixture of the two compounds (see Figure 7) assures us of their complete miscibility. Specifically, the collapse pressure increases with the mole fraction of $C_{18}OH$. Also, the limiting area per molecule in a given mixture ($A_{1,m}$) extrapolated from the high-pressure region to $\pi = 0$ decreases proportionally to the $C_{18}OH$ mole fraction in the films and can be expressed in terms of the limiting areas at $\pi = 0$ for pure $C_{18}Fc$ and $C_{18}OH$:

$$A_{1,m} = x_{C_{18}Fc}A_{1,C_{18}Fc} + x_{C_{18}OH}A_{1,C_{18}OH} \quad (3)$$

The calculated and experimentally determined values of $A_{1,m}$ for $x_{C_{18}Fc} = 0.3$ are 28.4 and 28 Å^2/molecule, and when $x_{C_{18}Fc} = 0.5$ they are 34.0 and 33 Å^2/molecule, respectively.

We will discuss the data in Figure 6 in view of the Cohen–Turnbull theory[8] of diffusion in hard-sphere fluids, which has been used before to analyze lateral diffusion in phospholipid monolayers and bilayers.[15] According to this model, molecules move with their gas-phase velocity (u) whenever a fluctuation of density creates a void in the cage of their residence. In the early version of this model,[8a] the authors assumed that the void volume has to exceed a certain critical value (v^*) on the order of molecular size for the diffusion coefficient to be above zero. The latter was then expressed by the following:

$$D = ga^*u\int_{v^*}^{\infty} p(v)\mathrm{d}v \quad (4)$$

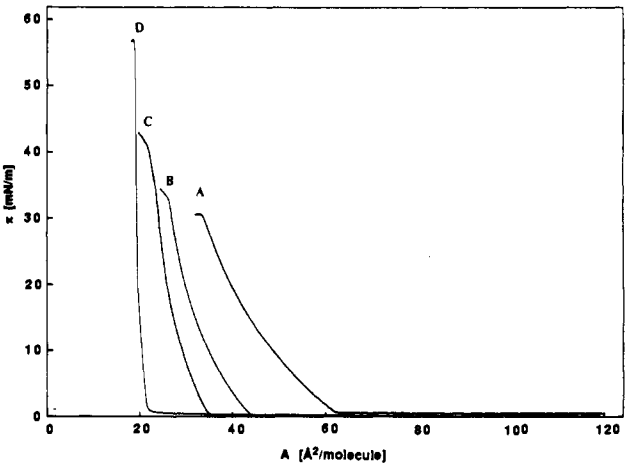

Figure 7. π–A isotherms of $C_{18}Fc$ + $C_{18}OH$ monolayers at the 0.05 M $HClO_4$ subphase. $C_{18}Fc$ mole fractions are A, 1.0; B, 0.5; C, 0.3; D, 0.0. T = 28 °C.

where g is a geometric factor, a^* is the mean displacement approximated by the molecular diameter and $p(v)$ is the probability of finding the free volume between v and $v + \mathrm{d}v$. The distribution of the total free volume is[8a]

$$p(v) = (\gamma/v_f)\exp(-\gamma v/v_f) \quad (5)$$

where v_f is the average free volume and γ is a numerical parameter between 0.5 and 1, introduced to correct for the overlap of free volume. The combination of eqs 4 and 5 gives

$$D = ga^*u\exp(-\gamma v^*/v_f) \quad (6)$$

Less well known is a more recent refinement of the free volume model, where Turnbull and Cohen expressed the diffusion coefficient by[8b]

$$D = gu\int_{v^*}^{\infty} p(v)f(v)a(v)\mathrm{d}v \quad (7)$$

In this version of the model, the average displacement ($a(v)$) was assumed to be a linear function of the free volume ($a(v) = \alpha v$). Also, a correlation factor for displacement ($f(v)$) was introduced to express whether the system behaves like a solid or whether it is "gaslike". $f(v)$ is unity for a random walk at $v > v^*$ and approaches 0 for the "solidlike" behavior at $v < v^*$. Using a step function approximation to $f(v)$, after the integration in eq 7, one obtains

$$D = gu\alpha(v^* + v_f/\gamma)\exp(-\gamma v^*/v_f) \quad (8)$$

This expression for the diffusion coefficient assumes the form of

(15) (a) Galla, H. J.; Hartmann, W.; Theilen, M.; Sackmann, E. *J. Membr. Biol.* **1979**, *48*, 215. (b) Peters, R.; Beck, K. *Proc. Natl. Acad. Sci. U.S.A.* **1983**, *80*, 7183. (c) Vaz, W. L. C.; Goodsaid-Zalduondo, F.; Jacobson, K. *FEBS Lett.* **1984**, *174*, 199. (d) Vaz, W. L. C.; Clegg, R. M.; Hallmann, D. *Biochemistry* **1985**, *24*, 781.

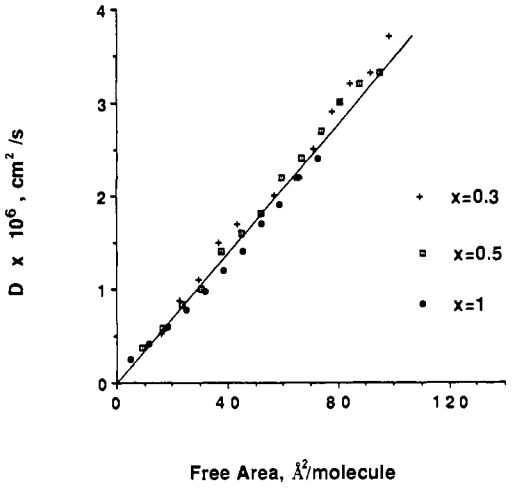

Figure 8. $C_{18}Fc$ lateral diffusion coefficients from Figure 6B vs average free area per molecule.

eq 6 for $v^* \gg v_f/\gamma$. However, for $v^* \ll v_f/\gamma$, it gives a direct proportionality of D vs v_f:

$$D = gu\alpha v_f/\gamma \tag{9}$$

In physical terms, the latter limit assumes that no minimum void volume is necessary for diffusion to take place and that the system is fluid and thus behaves randomly at all levels of void volume greater than zero: $f(v) = 1$ for $v > 0$. It is easy to show that eq 9 can be obtained directly from eq 7 by changing the limits of the integration to 0 to ∞.

The fit of the data in Figure 6B to eq 9 is quite apparent after one expresses the average area per molecule in terms of the free area ($A_f = A - A_0$; v_f now corresponds to A_f; see Figure 8). A_0 was obtained for each series of experiments in Figure 6B by extrapolating the data to $D = 0$. A good agreement was also found when these data were fit to eq 8. A two-parameter ($B = gu\alpha/\gamma$, $C = v^*\gamma$) nonlinear least-squares fit based on eq 8 rewritten as

$$D = B(C + A_f)\exp(-C/A_f) \tag{10}$$

gave, for the pure $C_{18}Fc$ series, $B = 3.2 \times 10^8$ s^{-1} and $C = 0.18$ Å^2. The low value of C warrants, indeed, the use of the simplified eq 9. Thus, the $C_{18}Fc$ monolayer behaves as a collection of hard disks in the entire range of concentrations examined in Figure 8.

The most important and revealing conclusion stemming from the data in Figure 8 is that the surface monolayers of pure $C_{18}Fc$ and its mixtures with $C_{18}OH$ remain fluid without exhibiting any phase transitions over a wide range of free areas. This behavior is observed at temperatures above ca. 25 °C. At lower temperatures as the $C_{18}Fc$ monolayer is expanded above approximately 62 Å^2/molecule, we observe an abrupt disappearance of the electrochemical current, which could signal an onset of a phase transition. Under the conditions of Figure 8, well-behaved 2D voltammograms with peak currents consistent with the data in Figure 8 can be recorded at $C_{18}Fc$ inverse concentrations as high as 250 Å^2/molecule. Beyond this point, less reproducible data are observed, suggesting a nonhomogeneous state of the monolayer. This aspect of the system's behavior will be discussed in a separate report.

An attempt to fit these results to the earlier formulation of the free volume model[8a] (eq 6) produced linear ln D vs $1/A_f$ plots only for values of the free area less than ca. 40 Å^2/molecule. A large positive deviation was observed when the monolayer was more expanded. A very similar characteristic was reported by Peters and Beck concerning lateral diffusion of a fluorescent lipid probe in dilauroylphosphatidylcholine monolayers at the air/water interface measured by fluorescence microphotolysis.[15b] Their values of D were very similar to ours for a given average free area per molecule, and we found that these also gave linear plots when replotted according to eq 9. When these two techniques are compared, it is interesting to point out that the electrochemical method of measuring translational diffusion in Langmuir monolayers is essentially free from convective interferences, since the water surface in the immediate vicinity of the electrode is shielded from such interferences and because the diffusion layer extends only a few μm away from the microband electrode. Such interferences may constitute a major difficulty in the fluorescence microphotolytic measurements.[15b]

Finally, we would like to discuss a mechanistic implication of these results. In principle, lateral 2D current measured in this experiment is proportional to the sum of contributions due to translational diffusion of $C_{18}Fc$ and to the lateral electron hopping between ferrocene and ferrocenium sites in the monolayer. The adherence of the data in Figure 8 to the free volume model over the entire range of concentrations provides a strong argument against participation of electron hopping in the overall current. Thus, electron hopping appears to be too slow to compete with physical diffusion even at the highest concentrations of $C_{18}Fc$, where translational diffusion is at its lowest level and where the proximity of the ferrocene sites maximizes the contribution of the electron transfer. Evaluation of D under these conditions allows us to estimate an expected value of the rate constant of the electron transfer, which would result in an electron hopping diffusion coefficient (D_e) matching the lowest measured value (D). Theoretical work of Andrieux and Savéant[16] and others[17] based on a stochastic model of diffusive propagation of electrons involving a series of electron-exchange reactions between neighboring reduction/oxidation centers led to the following expression for D_e:

$$D_e = {}^1/_6 k_{ex}\delta^2 C \tag{11}$$

where k_{ex} is a bimolecular electron-transfer rate constant, δ represents an average hopping distance, and C is the total concentration of the redox centers. A factor of $^1/_6$ is appropriate for a random electron propagation in 3D systems, such as polymer films incorporating redox species.[18] In such cases, k_{ex} and C bear their usual 3D units. Transposition of eq 11 to 2D systems was shown to be straightforward:[17c]

$$D_e = {}^1/_4 {}^{2D}k_{ex}\delta^2\Gamma^* \tag{12}$$

where 2D electron transfer rate constant $^{2D}k_{ex}$ is expressed in cm^2 mol^{-1} s^{-1} and Γ^* in mol cm^{-2}. (Units of D are, of course, invariant regardless of the dimensionality of a system.) One is then faced with a difficulty of comparing the calculated value of $^{2D}k_{ex}$ from eq 12 with 3D literature values. This problem can be handled in the framework of the precursor complex model of electron transfer, where briefly the observed bimolecular rate constant is expressed as a product of a unimolecular rate constant (k_{et} (s^{-1}) and a precursor complex "equilibrium constant" (K_p).[19]

$$k_{ex} = k_{et}K_p \tag{13}$$

For a pair of spherical reactants with no Coulombic repulsion involved in the formation of the precursor complex, K_p can be approximated by the following:[19]

$$K_p = 4\pi NR^2\delta R \tag{14}$$

N is Avogadro's number, R is the radius of an excluded volume encompassing both reactants or an internuclear distance between the reactants in the transition state, and δR is the "reaction zone thickness". This is the range of distance over which the electron is transferred with an appreciable rate (e.g., δR was assumed to be 0.6 Å for the ferrocene/ferrocenium precursor complex).[20] It

(16) Andrieux, C. P.; Savéant, J.-M. *J. Electroanal. Chem.* **1980**, *111*, 377.
(17) (a) Laviron, E. *J. Electroanal. Chem.* **1980**, *112*, 1. (b) Ruff, I.; Botar, L. *J. Chem. Phys.* **1985**, *83*, 1292. (c) Botar, L.; Ruff, I. *Chem. Phys. Lett.* **1986**, *126*, 348.
(18) Wilbourn, K. O.; Facci. J. S.; Murray, R. W. *Chem. Phys.* **1990**, *141*, 143.
(19) (a) Sutin, N. *Prog. Inorg. Chem.* **1983**, *30*, 441. (b) Hupp, J. T.; Weaver, M. J. *J. Electroanal. Chem.* **1983**, *152*, 1.
(20) (a) Gannett, T.; Milner, D. F.; Weaver, M. J. *J. Phys. Chem.* **1985**, *89*, 2787. (b) Nielson, R. M.; McManis, G. E.; Golovin, M. N.; Weaver, M. J. *J. Phys. Chem.* **1988**, *92*, 3441.

is apparent that the expression for K_p has units of volume per mole (geometrically, the volume involved is that of the "reaction zone"); thus, transposition of this expression into a 2D system gives

$$^{2D}K_p = 2\pi NR\delta R \quad (15)$$

and the 2D expression analogous to eq 13 is

$$^{2D}k_{ex} = k_{et}{}^{2D}K_p \quad (16)$$

In view of eqs 12-16, the relationship between k_{ex} and $^{2D}k_{ex}$ can be expressed by eq 17. Assuming a literature value of R (7.6 Å) for the ferrocene/ferrocenium precursor complex,[20] we obtained $k_{ex} = 6.4 \times 10^7$ M^{-1} s^{-1} as an expected value of the electron-transfer rate constant, which would lead to D_e equal to the lowest D observed in our experiments at the air/water interface. A

$$k_{ex} = {}^{2D}k_{ex}2R \quad (17)$$

literature value for the ferrocene/ferricenium rate constant in acetonitrile is 9.1×10^6 M^{-1} s^{-1}.[21] Direct comparison of these values is complicated by uncertainties stemming from solvent effects and other phenomena that cannot be evaluated precisely for the $C_{18}Fc$ system at the air/water interface. However, it is not surprising that the present measurements appear to reflect solely translational diffusion. Since the measurements of the electron transfer rate constant involving sites at the air/water interface could shed some light on solvation effects and reveal, potentially, orientational dependence of the electron transfer kinetics, we are currently pursuing various strategies aimed at restricting the rate of lateral diffusion in these types of systems in order to experimentally access the kinetics of electron self-exchange.

(21) Nielson, R. M.; McManis, G. E.; Safford, L. K.; Weaver, M. J. *J. Phys. Chem.* **1989**, *93*, 2152.

Conclusions

The main conclusions of this report can be summarized in the following points:

1. We have developed a microband electrode that can be used in electrochemical experiments at the air/water interface and demonstrated the application of electrochemical techniques in the measurements of the dynamics of 2D lateral diffusion in Langmuir monolayers.

2. Lateral diffusion of $C_{18}Fc$ at the air/water interface, alone and in mixtures with $C_{18}OH$, obeys a simple free area model in a broad range of surface concentrations, in which the diffusing molecules can be treated as hard disks with the surface area equal to the projected area of their head groups.

3. Above approximately 25 °C, the $C_{18}Fc$ monolayer remains fluid and does no exhibit phase transitions in the range of free areas of ca. 5-100 $Å^2$/molecule.

4. The magnitude of the $C_{18}Fc$ lateral diffusion coefficient of ca. 2×10^{-7} cm^2/s measured at the highest surface concentration attainable in these studies is sufficiently high as to eliminate any contribution to the lateral current due to electron hopping in this 2D network of the redox sites.

Acknowledgment. We gratefully acknowledge the National Science Foundation for supporting this research under Grant CHE-8807846. We thank Professor K. B. Whaley and Dr. C. A. Goss for many insightful discussions. E.M.L. acknowledges and thanks the Rothschild Foundation for a postdoctoral fellowship (1988-1989).

Comparative Molecular Mechanics Study of the Low-Spin Nickel(II) Complexes of an Extended Series of Tetraaza Macrocycles

Kenneth R. Adam, Michael Antolovich, Larry G. Brigden, and Leonard F. Lindoy*

Contribution from the Department of Chemistry and Biochemistry, James Cook University, Queensland 4811, Australia. *Received July 23, 1990*

Abstract: Molecular mechanics calculations of metal complex structures are often not straight forward because of uncertainties concerning the appropriate force-field parameters for structural elements involving the metal. A systematic study aimed at extending the Allinger MM2 force field for use with N_4-macrocyclic complexes of low-spin Ni(II) is reported. Although molecular mechanics investigations of particular low-spin Ni(II) complexes of tetraaza macrocycles have been performed previously, no calibration of the force field for such complexes with a wide range of compounds of this type has been reported. X-ray data for twenty low-spin Ni(II) complexes incorporating solely sp^3 nitrogen donors and six complexes also containing sp^2 nitrogens have been used in the calibration of the extended force field. Inclusion of an out-of-plane bending term, which restricts the degree to which the Ni(II) atom can deviate from the least-squares plane of the donor atoms, was generally beneficial in modeling the respective coordination planes. The application of the extended force field to the re-examination of the configurational isomers of $[Ni(cyclam)]^{2+}$ and their N,N,N,N-tetramethylated derivatives is reported.

Since the introduction of the molecular mechanics procedure for organic molecules,[1] there has been continuing development of the method toward the modeling of other types of compounds,[2] including transition-metal complexes.[3,4] For example, much attention has been given to the conformational analysis of the

(1) Allinger, N. L. *Adv. Phys. Org. Chem.* **1976**, *13*, 1. Burkert, U.; Allinger, N. L. *Molecular Mechanics*; American Chemical Society: Washinton, DC, 1982; p 1ff and references therein. Allinger, N. L. *J. Am. Chem. Soc.* **1977**, *99*, 8127.

(2) Weiner, S. J.; Kollman, P. A.; Case, D. A.; Singh, U. C.; Ghio, C.; Alagona, G.; Proteta, S.; Weiner, P. *J. Am. Chem. Soc.* **1984**, *106*, 765. Grootenhuis, P. D. J.; Kollman, P. A. *J. Am. Chem. Soc.* **1989**, *111*, 2152, 4046. Andreetti, G. D.; Ori, O.; Ugozzoli, F.; Alfieri, C.; Pochini, A.; Ungaro, R. J. *Incl. Phenom.* **1988**, *6*, 523. Kollman, P. *Acc. Chem. Res.* **1985**, *18*, 105 and references therein.

0002-7863/91/1513-3346$02.50/0